Quantum Control in Macroscopic Path Length Systems

Colin J. Fuller

Submitted in Partial Fulfillment
of the Requirements of the
Degree of
Bachelor of Arts

Department of Chemistry
of
Princeton University

May 1, 2006

I hereby declare that I am the sole author of this thesis, and that this thesis represents my own work in accordance with University regulations.

Colin J. Fuller

Acknowledgements

I would like to gratefully acknowledge the help and support of Professor Herschel Rabitz and graduate students Jonathan Roslund and Matthias Roth, all of whom were very generous with their time and talents, and without whose help I would not have been able to work on this project.

Abstract

Quantum control aims to control chemical reactions, excitations, and other processes using shaped laser pulses, but in order for it to be of any practical application, it must be able to control these processes in a relatively large volume of material. To date, most experimental quantum control work has been done on the microscale. This study aims to investigate whether quantum control can be extended to larger volumes and the mechanism by which control is achieved in these larger volumes. Using a tube of fluorescent laser dye as a model quantum system, it is seen that fluorescence can be optimized for different locations along the tube and an investigation into the solutions of the control problem is made.

Introduction

One of the main problems the field of quantum control is currently facing is that the technique has not yet been applied on a practical scale. Most work to date has been theoretical and that work that has been done in the lab has generally been done on a microscale. From the perspective of a chemist, the eventual practical goal of quantum control is to be able to bring about any reasonable chemical reaction in the lab using laser pulses specifically shaped for that purpose. For this to work, it is necessary to have quantum control work on macroscale volumes of whatever system is to be controlled.

The problem with control on the macroscale is that the interaction of the pulse with the medium will cause the pulse to be reshaped, through absorption, dispersion, or nonlinear effects, so that the pulse that the system "sees" near the beginning of the pulse's path is not the same one that it "sees" near the end of the path.

Wang and Rabitz [1] investigated this problem theoretically, and showed that for an ideal three level system, it is possible to control population transfer among these states over an arbitrary distance when the reshaping of the pulse is taken into account. A previous unpublished study from this lab confirmed that this sort of optimization was experimentally possible. The current study aims to duplicate that result and make a more complete characterization of that phenomenon.

Materials and Methods

The experimental system used to model an ideal three-level system used in the theoretical investigation is a tube filled with a laser dye dissolved in ethanol. The laser dye is excited in a two photon process and fluoresceses at a higher frequency than that either photon in the initial excitation. A femtosecond pulsed laser with wavelength near that required for the two photon excitation is used to create a pulse that is passed through a pulse shaper that uses liquid crystals to modulate the phase of the different frequency components of the pulse. These phase-modulated components are then recombined and passed through the tube of dye. The fluorescence produced by a given pulse is measured by photodiodes, and this fluorescence is used as a measure of population transfer in the system.

The particular dye used is Coumarin 102, dissolved in 100% ethanol at a concentration of 5g/L, which is near the solubility point of the dye. A cylindrical optical glass tube of 10cm path length and 1cm diameter was filled with this solution, sealed, and fixed in the path of the laser beam. Additionally, a frequency-resolved optical gating (FROG) device was set up to be able to characterize each pulse in the time and frequency domain both before and after passing through the tube.

Figure 1 gives a schematic view of the experimental setup.

Each experiment progressed by first selecting a fitness function of the signals from each detector and putting this function into a genetic algorithm.

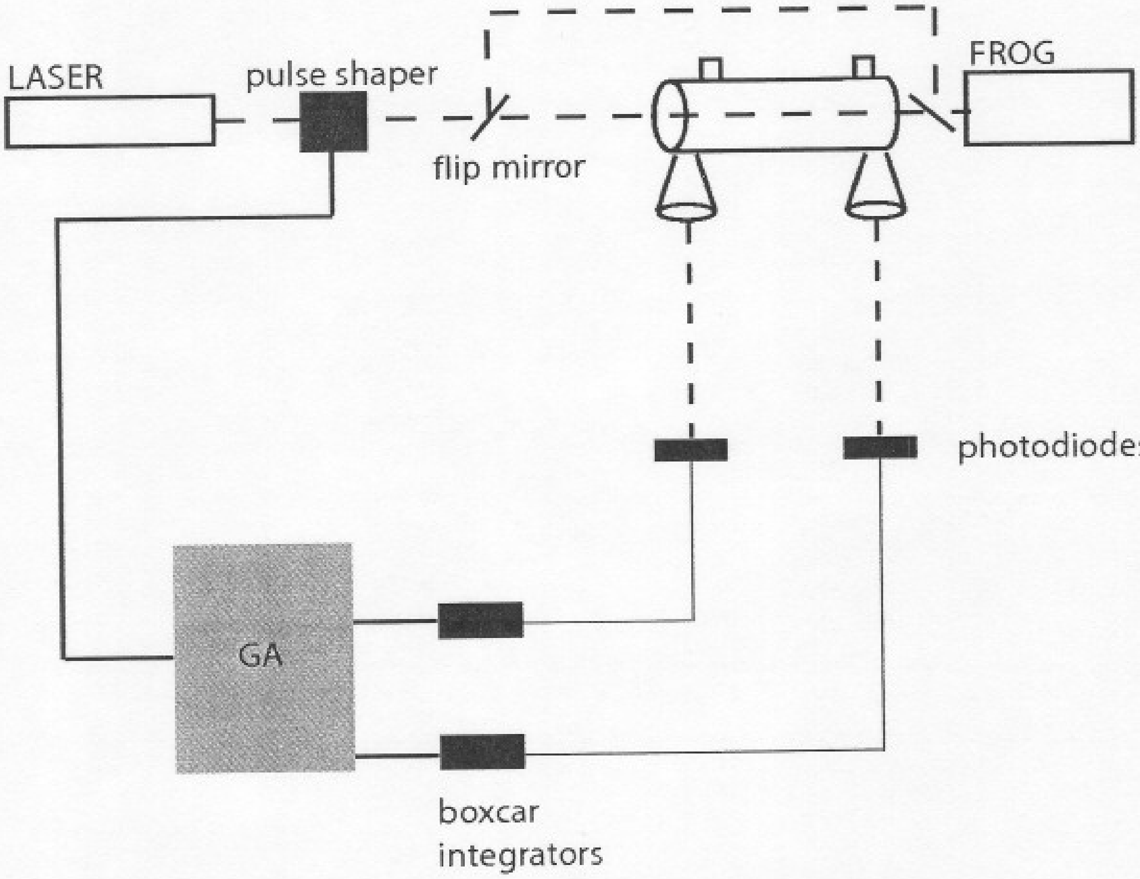

Figure 1: schematic of the experimenal setup.

The genetic algorithm would then randomly select shapes for pulses, and then recombine and mutate them based on their fitness in order to attempt to maximize the fitness function. Then, the optimal pulse found after optimization was sent to the FROG both before and after being passed though the tube, and the pulse characterized.

Results

A basic set of 5 fitness functions was used to perform optimizations and take a FROG trace before and after the tube. These fitness functions are summarized in table 1. Essentially, there is one that asks the algorithm to maximize the signal at each detector, one that asks to optimize the sum of the signals from the detectors, and one that asks to maximize the signal at each detector while minimizing the signal at the other.

The resulting near-optimal pulses were then put through the FROG, and subsequently the temporal field and phase and spectral field and phase extracted from the FROG trace. The results for each fitness function are presented in figures 2, 3, 4, 5, 6.

Analysis and Conclusions

Because of the positioning of the detectors, it is reasonable to assume that the pulse characterized before the tube is approximately the pulse that the front

Cost Function Number	Description	Function Form
1	maximize front detector	$F(S_1, S_2) = S_1$
2	maximize rear detector	$F(S_1, S_2) = S_2$
3	maximize sum of detectors	$F(S_1, S_2) = S_1 + S_2$
4	maximize front, minimize rear	$F(S_1, S_2) = \frac{S_1}{max(0.05, S_2)}$
5	maximize rear, minimize front	$F(S_1, S_2) = \frac{S_2}{max(0.10, S_1)}$

Table 1: fitness functions used for optimizations. In functions 4 and 5, a lower bound was put on the value of the denominator to reduce the effects of random noise; as the signal of the denominator approaches zero, the fitness goes to infinity infinitely fast. Thus, a noisy reading that put the denominator very close to zero could greatly skew the result. Putting in the lower bound helped to avoid this problem.

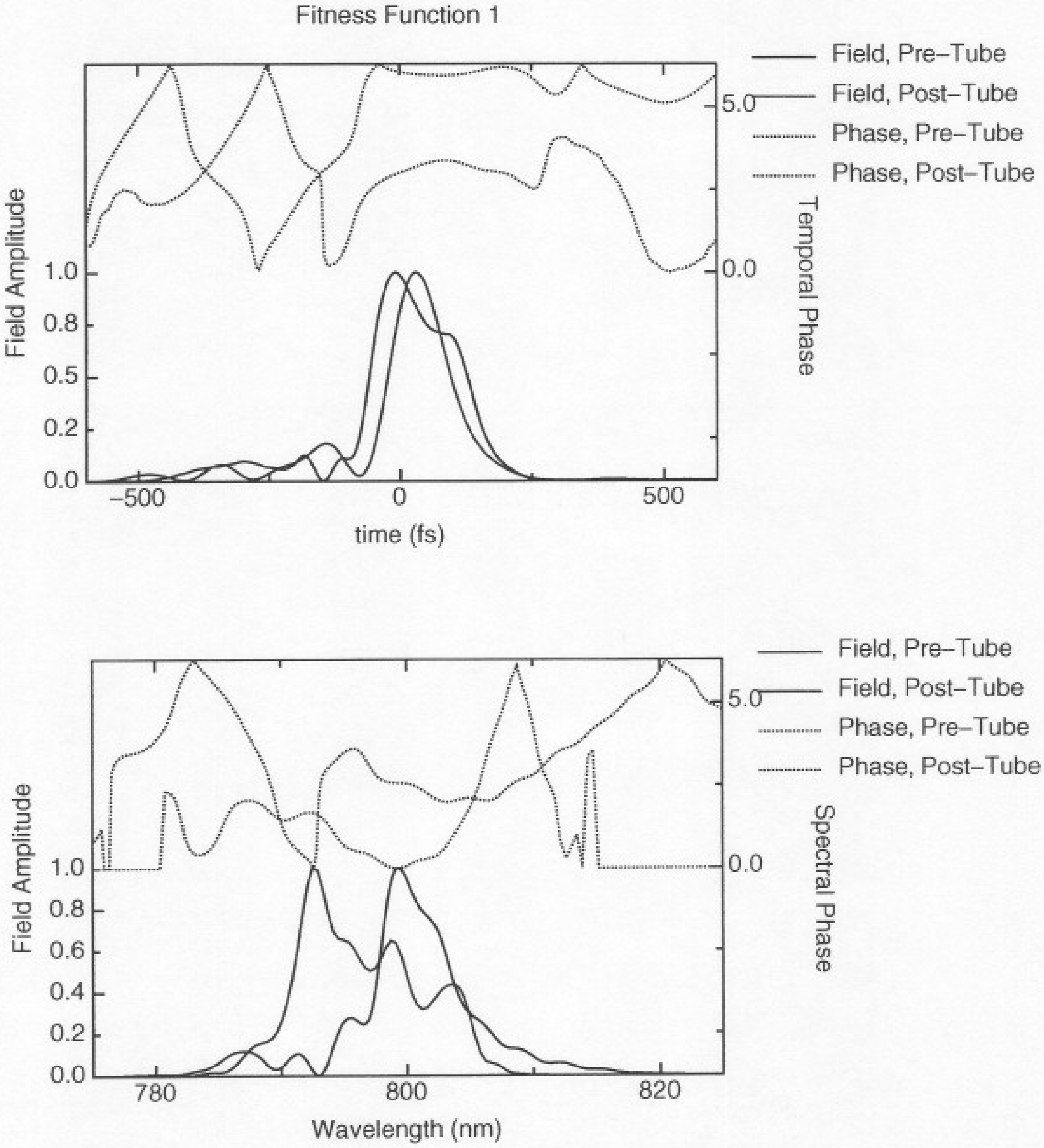

Figure 2: Characterized optimal pulse for fitness function 1 (optimized front detector). Amplitude units are arbitrary and normalized for each pulse separately.

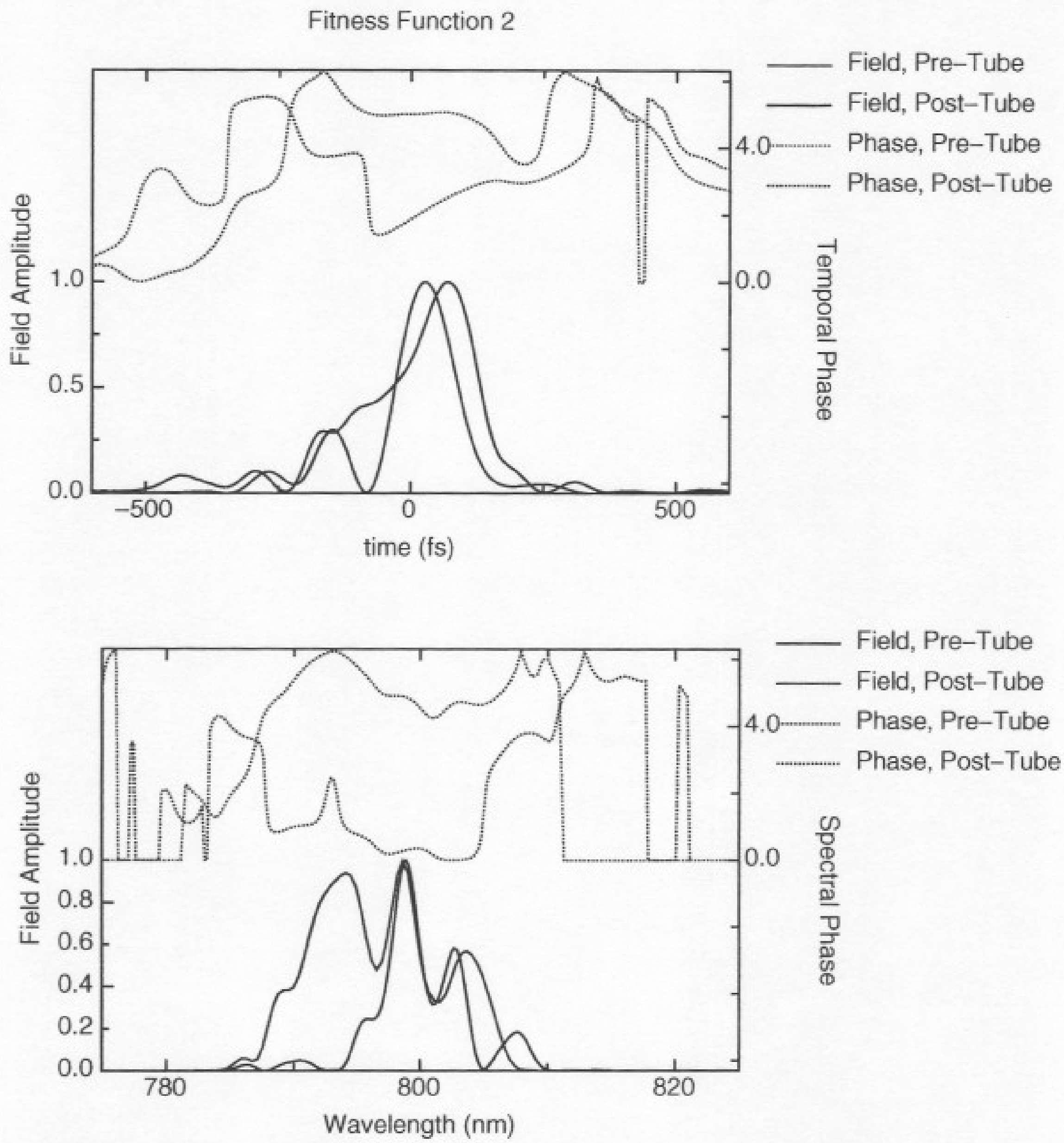

Figure 3: Characterized optimal pulse for fitness function 2 (optimized rear detector). Amplitude units are arbitrary and normalized for each pulse separately.

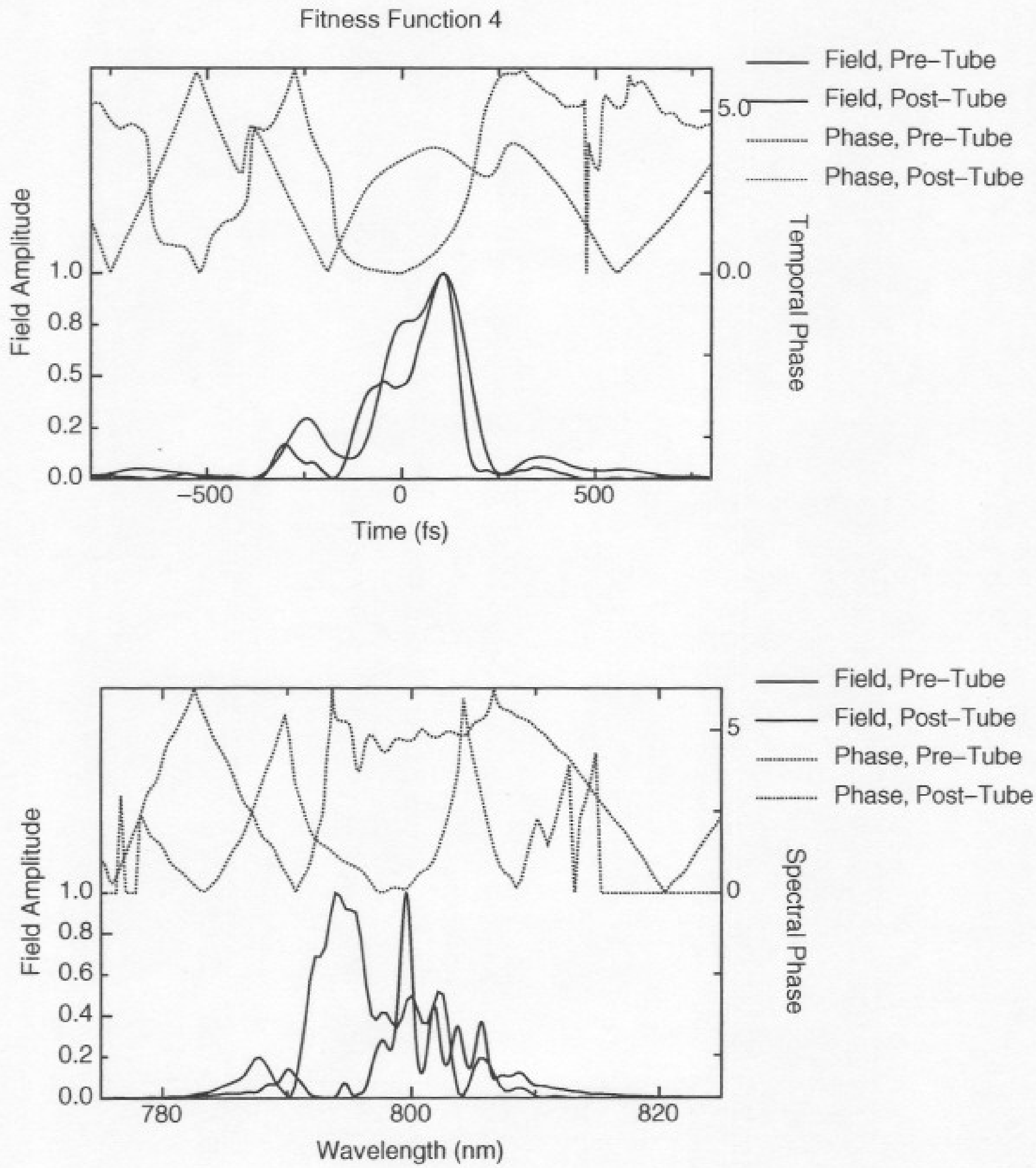

Figure 4: Characterized optimal pulse for fitness function 3 (optimized sum of detectors). Amplitude units are arbitrary and normalized for each pulse separately.

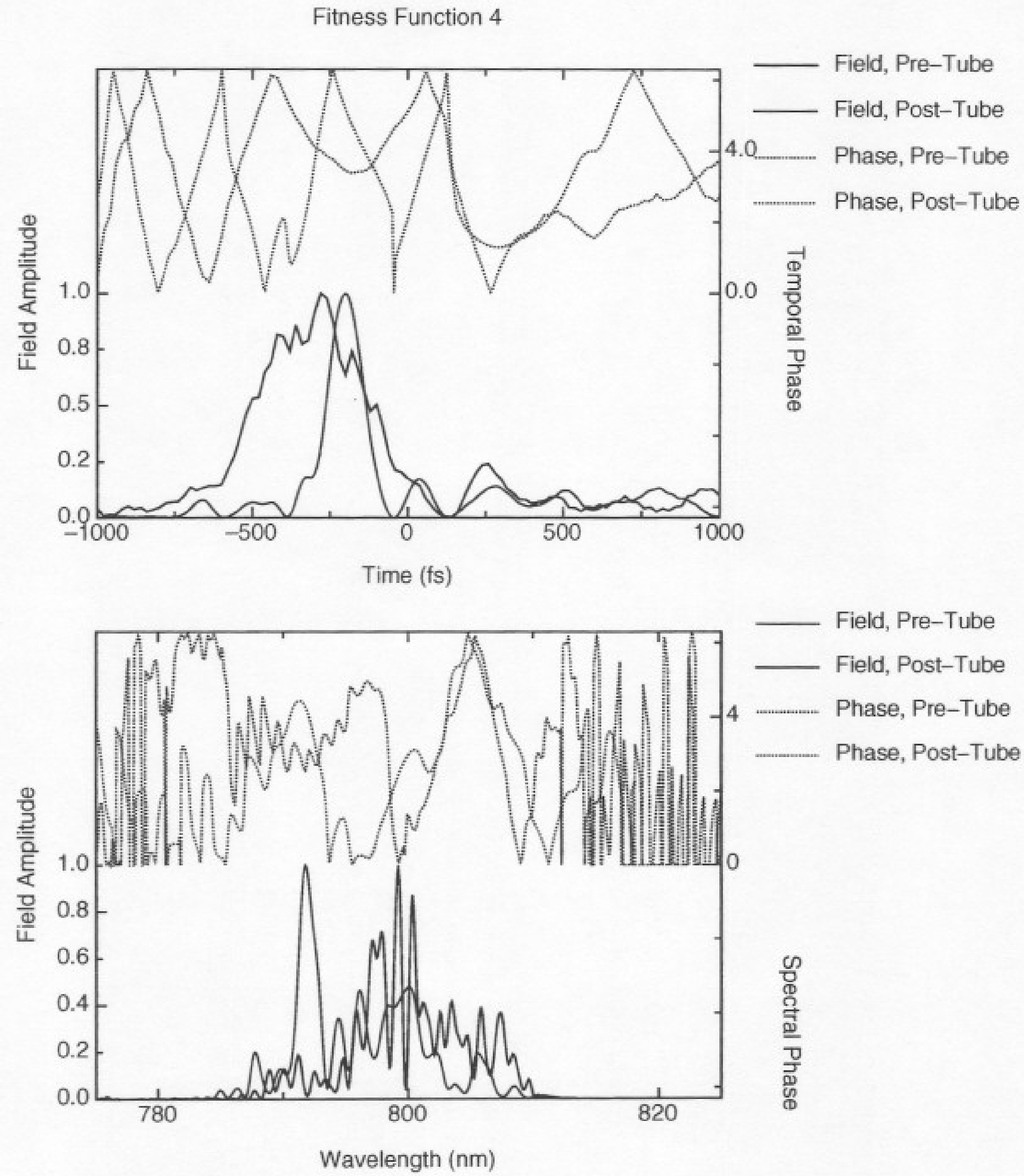

Figure 5: Characterized optimal pulse for fitness function 4 (optimized ratio front/rear detectors). Amplitude units are arbitrary and normalized for each pulse separately.

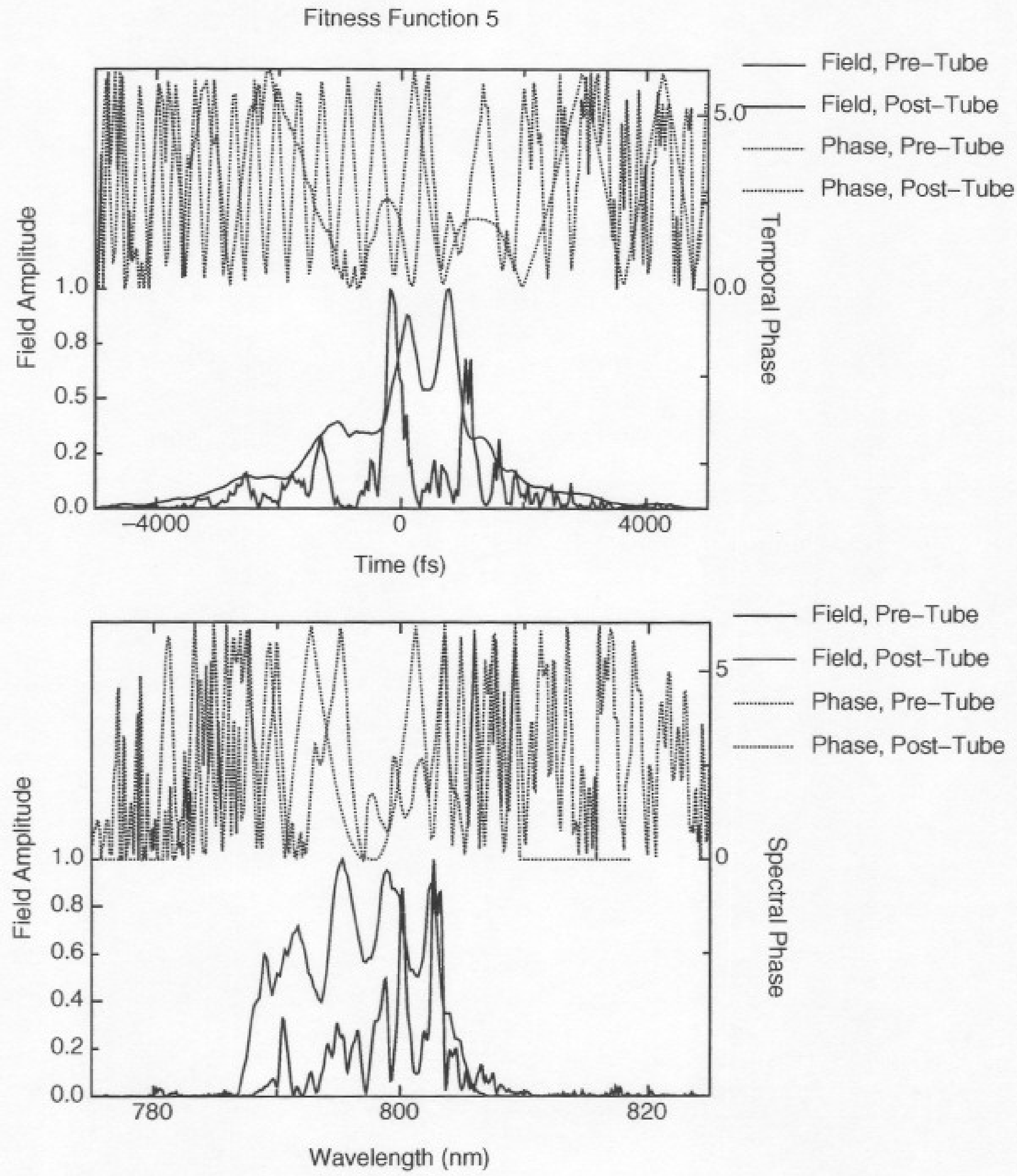

Figure 6: Characterized optimal pulse for fitness function 5 (optimized ratio rear/front detectors). Amplitude units are arbitrary and normalized for each pulse separately.

detector sees, and that the pulse characterized after the tube is approximately the pulse that the rear detector sees. One characteristic difference between the post-tube pulse and the pre-tube pulse is that the post-tube pulse is always redshifted with respect to the pre-tube pulse. This is sensible; the unshaped laser pulse has a spectrum centered at 794nm, and the coumarin dye absorbs slightly more to the blue than this. Thus, if the light on the bluer side of the spectrum is absorbed by the dye solution through the two-photon excitation, the remaining light at the end of the tube will be centered more to the red end of the spectrum.

A second observation from these data is that for fitness functions 1-3, which are simple optimizations, the pulse spectral phase near the detector being optimized is relatively slowly varying over the bandwidth of the pulse. Theory predicts that the optimal solution to the two photon process is a bandwidth-limited pulse (that is, a pulse with flat spectral phase), and the solutions found are not terribly inconsistent with that notion.

Additionally, where the algorithm was asked to increase one detector's signal at the expense of the other, the optimal pulse found was nontrivial. In the case of both fitness functions 4 and 5, the pulse measured nearer the detector to be maximized was qualitatively sharper than the pulse measured nearer the detector to be minimized. Since a bandwidth-limited pulse is qualitatively sharp, this makes some sense.

To make this observation quantitative, the FWHM time - FWHM bandwidth product was calculated for each pulse. The results are tabulated in table 2. (Note that the uncertainty principle states that $\Delta t \Delta \omega \sim 1$.)

For a laser pulse interacting with an isotropic medium like an ethanolic solution, higher order interactions only occur at third order and above due to symmetry. With sufficient laser power and focusing of the beam, white light generation and self-focusing (both third order effects)were observed. Using a neutral density filter, the power of the laser beam going through the tube was reduced so that these effects were no longer apparent to any appreciable extent, and the data reported here reflect experimental conditions with no third order effects.

The conclusion we can draw from these data is that to achieve optimization at a given location, the genetic algorithm converges to a pulse that after reshaping becomes as close to bandwidth-limited as possible at that location. When asked to maximize the signal at one point and minimize it at another, the algorithm converges to a pulse that is as far from the bandwidth limited pulse as possible at the detector to be minimized and as close as possible to it at the detector to be maximized.

This is a sensible and somewhat intuitive solution to the problem of quantum control over macroscopic path length systems. A key next step to a deeper understanding of this problem is integrating the experiments with theoretical-computational treatments of the same problem already being studied by this lab. This combination should lead to some greater insight into the exact mechanisms by which the pulses are reshaped and perhaps suggest new practical applications of quantum control.

Fitness Function	Front time-bandwidth product	Rear time-bandwidth product
1	2.94	3.06
2	4.65	2.55
3	7.01	0.44
4	0.61	4.29
5	50.04	13.75

Table 2: time-bandwith products (using FWHM values) for each pulse. These follow the general property that if one detector is being optimized, the time-bandwidth product for the corresponding pulse is smaller, as would be expected for the bandwidth-limited pulse solution.

References

[1] Wang, N. J.; Rabitz, H. *J Chem Phys* **1996**, *104*, 1173-1178.